



OPEN ACCESS

EDITED BY

Vishal Govind Rao,
Indian Institute of Technology Kanpur,
India

REVIEWED BY

Jan Krajczewski,
University of Warsaw, Poland
Sarthak Mandal,
National Institute of Technology, India

*CORRESPONDENCE

Sammy W. Verbruggen,
sammy.verbruggen@uantwerpen.be

SPECIALTY SECTION

This article was submitted to
Photocatalysis and Photochemistry,
a section of the journal
Frontiers in Chemistry

RECEIVED 07 July 2022

ACCEPTED 26 August 2022

PUBLISHED 12 September 2022

CITATION

Dingenen F, Borah R, Ninakanti R and
Verbruggen SW (2022), Probing oxygen
activation on plasmonic photocatalysts.
Front. Chem. 10:988542.
doi: 10.3389/fchem.2022.988542

COPYRIGHT

© 2022 Dingenen, Borah, Ninakanti and
Verbruggen. This is an open-access
article distributed under the terms of the
[Creative Commons Attribution License
\(CC BY\)](https://creativecommons.org/licenses/by/4.0/). The use, distribution or
reproduction in other forums is
permitted, provided the original
author(s) and the copyright owner(s) are
credited and that the original
publication in this journal is cited, in
accordance with accepted academic
practice. No use, distribution or
reproduction is permitted which does
not comply with these terms.

Probing oxygen activation on plasmonic photocatalysts

Fons Dingenen^{1,2}, Rituraj Borah^{1,2}, Rajeshreddy Ninakanti^{1,2,3}
and Sammy W. Verbruggen^{1,2*}

¹Department of Bioscience Engineering, University of Antwerp, Sustainable Energy, Air & Water Technology (DuEL), Antwerp, Belgium, ²Nanolab Center of Excellence, University of Antwerp, Antwerp, Belgium, ³Department of Physics, Electron Microscopy for Material Science, University of Antwerpen, Antwerp, Belgium

In this work we present an assay to probe the oxygen activation rate on plasmonic nanoparticles under visible light. Using a superoxide-specific XTT molecular probe, the oxygen activation rate on bimetallic gold-silver “rainbow” nanoparticles with a broadband visible light (> 420 nm) response, is determined at different light intensities by measuring its conversion into the colored XTT-formazan derivative. A kinetic model is applied to enable a quantitative estimation of the rate constant, and is shown to match almost perfectly with the experimental data. Next, the broadband visible light driven oxygen activation capacity of this plasmonic rainbow system, supported on nano-sized SiO₂, is demonstrated towards the oxidation of aniline to azobenzene in DMSO. To conclude, a brief theoretical discussion is devoted to the possible mechanisms behind such plasmon-driven reactions.

KEYWORDS

surface plasmon resonance (SPR), photocatalysis, probe, Kinetics, oxygen activation

1 Introduction

Direct plasmonic photocatalysis is a process in which plasmonic metal nanoparticles act as both the catalytic active site as well as the light absorber simultaneously. Recent reports have shown that it is possible to use visible light to fuel different chemical transformations on plasmonic nanoparticles directly, without the requirement of a photoactive semiconducting substrate (Brongersma et al., 2015; Zhou et al., 2021). These include the degradation of different organic dyes like methylene blue (Chen et al., 2012; Pincella et al., 2014; Boerigter et al., 2016) and sulforhodamine-B (Zhu et al., 2009; Chen et al., 2010), mineralization of formaldehyde (Chen et al., 2008; Kale et al., 2014), selective reduction of various nitroaromatics to form their corresponding azo-compounds (Zhu et al., 2010), ethylene epoxidation (Christopher et al., 2011), selective oxidation of alcohols (Zhang et al., 2012), esterification of aldehydes and alcohols (Zhang et al., 2014), selective CO₂ hydrogenation (Zhang et al., 2017; Inoue et al., 2019; Yu and Jain, 2019) and cross-coupling reactions (Wang et al., 2013; Xiao et al., 2014b; Zhao et al., 2016). More recently, further tuned hybrid systems occurred, where several metals are alloyed or used in a core-shell configuration, even with less plasmonic, more catalytically active metals (e.g., Ru, Pt, and Pd) in antenna-reactor systems (Swearer et al., 2016; Robotjazi et al., 2020; Zhou et al., 2020). Apart from its renewable character, the use of

sunlight allows chemical transformations to take place at ambient temperature and pressure. This substantially reduces equipment cost and increases catalyst operation time due to the less harsh reaction conditions (Lang et al., 2014; Peiris et al., 2016; Wu et al., 2017). The Surface Plasmon Resonance (SPR) effect can also selectively channel photon energy, ultimately facilitating the rate-limiting step (Kale et al., 2014).

Most of the oxidative chemical reactions as those listed above, involve activation of oxygen as a key step in the reaction mechanism (Chen et al., 2010; Wittstock et al., 2010; Christopher et al., 2011; Zhang et al., 2012; Huang et al., 2014). Traditionally, these oxidation reactions are carried out using stoichiometric quantities of toxic inorganic reagents that often entail a high waste disposal cost. Alternatively, by solely using molecular oxygen as primary oxidant, a high atom economy and low waste cost can be achieved. In addition, no hazardous inorganic reagents are needed (Punniyamurthy et al., 2005; Campbell and Stahl, 2012; Ali et al., 2014; Lang et al., 2014). It has already been demonstrated that oxygen can be activated on plasmonic nanoparticles by exploiting the SPR effect, where excited 'hot' electrons are formed by visible light illumination that are subsequently transferred to O₂ molecules adsorbed on the nanoparticle surface, as studied by surface-enhanced Raman spectroscopy (SERS) (Huang et al., 2014; Wang et al., 2014; Da Silva et al., 2015; da Silva et al., 2016), electron paramagnetic resonance spectroscopy (EPR) (Gao et al., 2014; Long et al., 2014; Sakamoto et al., 2015; Di et al., 2016; Wen et al., 2016), UV-VIS spectroscopy (Pasparakis, 2013; Wen et al., 2016), phosphorescence spectroscopy (Vankayala et al., 2011, 2013; Gao et al., 2014), density functional theory (DFT) calculations (Christopher et al., 2011; Zhao et al., 2014, 2016) and kinetic isotope experiments (Christopher et al., 2011).

In this study a wet-chemical probing technique is presented to monitor plasmonic oxygen activation directly in the reaction solution, a convenient experimental tool that has not been applied in this context before. To that end, XTT {2,3-bis(2-methoxy-4-nitro-5-sulphophenyl)-5-[(phenylamino)carbonyl]-2H-tetrazolium, sodium salt} is used as a probe molecule to examine the charge transfer process of hot electrons to dissolved oxygen. XTT is readily reduced by superoxide anions (O₂⁻) to form its corresponding formazan dye, that shows a strong visible light absorption (Oritani et al., 2004; Li et al., 2013; Azócar et al., 2019). This distinct color change associated with the tetrazolium/formazan redox couple, forms the basis of the existing applications as indicators in cell biology (Seidler, 1991; Berridge et al., 2005; Popescu et al., 2015). One of these applications is the quantitative detection of superoxide anions (O₂⁻), formed by the one-electron reduction of O₂, in biological systems. Tetrazolium salts are therefore commonly used in cell ageing or toxicity studies, as reactive oxygen species play an important role in such processes. Another application is as indirect assay of the enzyme activity of superoxide dismutase

(Sutherland and Learmonth, 1997; Oritani et al., 2004). It has also been applied to detect superoxide in different non-biological systems such as on irradiated TiO₂ (Goto et al., 2004; Popescu et al., 2015), fullerenes (Yamakoshi et al., 2003; Hotze et al., 2008) or to study chemiluminescence in carbon nanodots (Xue et al., 2011), amongst others. The present work shows the applicability of the XTT assay in (broadband) plasmonic catalysis to assess the oxygen activation rate during the reaction. By carefully evaluating the impact of operational parameters such as irradiation intensity, and photobleaching rate, a kinetic model is applied that enables a facile, quantitative estimation of the oxygen activation efficiency. As a proof of concept, the direct plasmonic photocatalytic oxidation of aniline to azobenzene (AB) is used to evaluate the oxygen activation efficiency of a broadband plasmonic rainbow photocatalyst.

2 Materials and methods

2.1 Plasmonic rainbow photocatalyst synthesis

The rainbow photocatalyst synthesis is already described in previous work (Verbruggen et al., 2016; Dingenen et al., 2021). In short, colloidal Au_xAg_(1-x) nanoparticles of different sizes and compositions (x varying from 0.2 to 1) were prepared following a modified Turkevich synthesis (Turkevich et al., 1951). Here, appropriate amounts of 0.01 M HAuCl₄·3H₂O (Sigma-Aldrich, > 99.9%) and 0.01 M AgNO₃ (Sigma-Aldrich, > 99%) precursor solutions were mixed, stirred vigorously and brought to boil. Then, 1 ml of a freshly prepared 1 wt% sodium citrate (Sigma-Aldrich, 99%) solution was quickly added as stabilizer and reducing agent. After boiling for 30 min, the reaction mixture was quenched in an ice bath. The rainbow sample was prepared by mixing equal amounts of the nine different colloidal solutions. The plasmonic bimetallic nanoparticles were subsequently deposited on silica nanopowder (Sigma-Aldrich, primary particle size 12 nm, 99.8%) by photoimpregnation. An appropriate amount of SiO₂ nanopowder was added to the colloidal rainbow solution under vigorous stirring and UVA illumination (Philips Cleo UVA, 25 W, 365 nm) for 90 min, so a total nominal metal loading of 1.5 wt% was achieved. The resulting suspension was centrifuged (15 min; 10,000 g), washed and dried overnight at 278 K. The supernatant after centrifugation was completely colorless, indicating all nanoparticles were effectively deposited on the SiO₂ substrate. UV-VIS absorption spectra of the colloidal nanoparticle solutions were recorded using a Shimadzu UV-VIS 2600 double beam spectrophotometer. The powder samples were characterized on the same apparatus, equipped with a 60 mm BaSO₄ coated ISR-2600 integrating sphere. For more detailed characterization of the bimetallic rainbow nanoparticles themselves (size determination, electron

microscopy and elemental analysis), we kindly refer the reader to our previous study (Verbruggen et al., 2016).

2.2 XTT assay

To monitor the oxygen activation efficiency (O_2^- formation) of the SiO_2 supported pure plasmonic rainbow photocatalyst, XTT was used as a probe molecule as it reacts with superoxide anions to form its corresponding colored formazan dye. 5 mg of the photocatalyst powder was suspended in a XTT sodium salt solution (10 ml, 0.1 mM, Sigma-Aldrich, $\geq 90\%$) in DMSO (dimethyl sulfoxide, Emplura, 99.0%) in a glass reactor vessel containing a screw cap (total volume of 11.3 ml) with airtight septum. The resulting suspension was purged with oxygen (5 min, 50 ml min^{-1}) to ensure oxygen saturation. The reaction vessel was subsequently illuminated with solely visible light using a 300 W Xe source (Oriel Instruments) equipped with a 420 nm cut-on colored glass long-pass filter. At different time intervals, 0.5 ml aliquots of the reaction mixture were taken and centrifuged at 14,800 rpm for five minutes to ensure complete catalyst separation. The resulting supernatant was analyzed using UV-VIS. The intensity of the Xe source was measured with a calibrated intensity spectrometer (Avantes Avaspec 3648). Absolute irradiance was subsequently calculated by integrating the intensity from 400 nm–800 nm.

2.3 Plasmon mediated oxidation of aniline

In a typical experiment, catalyst powder (25 mg) was suspended in an aniline solution (10 ml, 0.5 mM, Sigma-Aldrich, $\geq 99.5\%$) in DMSO in the airtight glass reaction tube. The resulting suspension was purged with O_2 (5 min, 50 ml min^{-1}) to ensure the reaction mixture was saturated with oxygen. The reaction vessel was subsequently illuminated with solely visible light using the same light source and filter as described above. During the reaction, 0.5 ml aliquots were taken at different time intervals and centrifuged for five minutes at 14,800 rpm to completely separate the catalyst. The resulting supernatant was analyzed by UV-VIS spectroscopy.

3 Results and discussion

3.1 Plasmonic photocatalyst

A plasmonic broadband “rainbow” system is synthesized based on earlier work that demonstrated the simultaneous absorption of multiple wavelengths over a broad range of the visible light spectrum (Verbruggen et al., 2016). In brief, the system consists of $Au_xAg_{(1-x)}$ bimetallic nanoparticles with x ranging from 0.2 to 1. Equivalent amounts of these particles

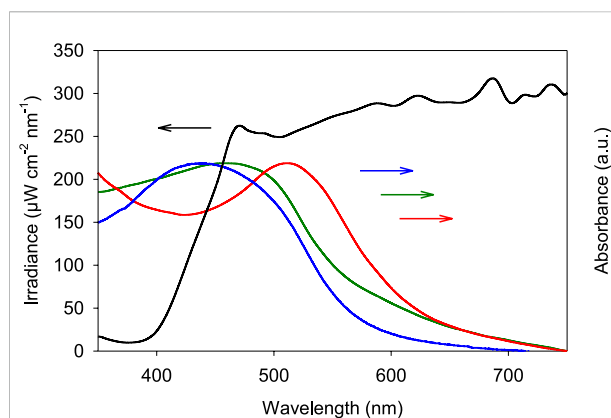


FIGURE 1

Intensity profile of the 300 W Xe lamp equipped with a 420 nm cut-on filter (black curve), liquid UV-VIS absorption spectrum of the unsupported colloidal rainbow mixture in water (blue), powder UV-VIS absorption spectrum of the plasmonic rainbow sample on SiO_2 (green) and the plasmonic rainbow sample on SiO_2 suspended in DMSO (red).

are mixed together to obtain the rainbow sample, that is characterized by a broad visible light absorption band (Figure 1). The particles are deposited on a non-photoactive SiO_2 support (12 nm nanopowder, Sigma-Aldrich) at a total metal loading of 1.5 wt%. Although it has been shown that unsupported plasmonic nanoparticles can catalyze reactions, their stability under these conditions remains troublesome, hence the reason for selecting SiO_2 as support. Furthermore, it strongly facilitates recovery and recyclability of the catalyst post-reaction (Lang et al., 2014; Xiao et al., 2014a). Figure 1 shows the diffuse reflectance UV-VIS absorption spectra of the resulting supported rainbow catalyst on SiO_2 . After depositing the nanoparticles on SiO_2 a red-shift is observed that can be explained by the higher refractive index of the SiO_2 support compared to water. In this work we used SiO_2 nanopowder with a crystallite size of 12 nm as the support. This way the resulting catalyst can be finely dispersed in liquid media at low concentrations, even enabling direct UV-VIS absorption measurements without the need for particle separation. Figure 1 also shows the absorption spectrum of the rainbow catalyst suspended in dimethyl sulfoxide (DMSO), that is used as solvent in both the probe reaction for determining the oxygen activation efficiency as well as the oxidation reaction of aniline. Because of the difference in refractive index between DMSO, water and air ($n_{DMSO} > n_{water} > n_{air}$) the SiO_2 supported rainbow photocatalyst suspended in DMSO experiences an additional red-shift, thereby well overlapping with the intensity spectrum of the light source (300 W Xe source with 420 nm cut-on filter, Newport). For more detailed characterization of the bimetallic rainbow nanoparticles themselves (size determination, electron

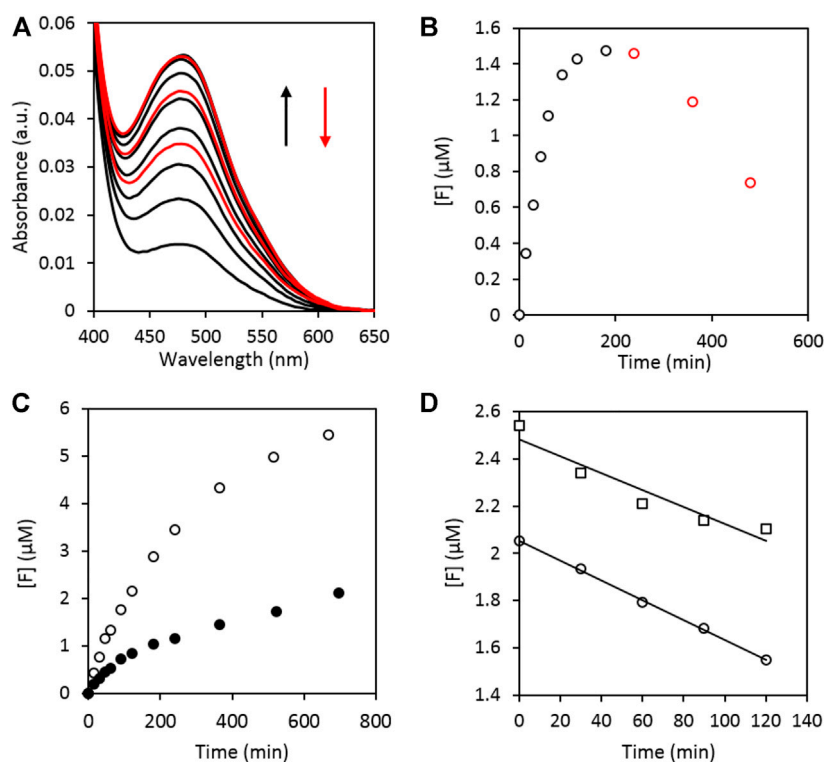


FIGURE 2

A) UV-VIS absorption spectra of the illuminated reaction mixture taken at different time intervals showing the formation of XTT formazan with λ_{max} at 480 nm. The absorbance increases during the first 180 min of illumination (black curves) after which the absorption band starts to decrease again (red curves). **(B)** Time dependent change of the formazan concentration ([F]) of **(A)**. The values were corrected for the initial conversion occurring during sample preparation. **(C)** Difference in formazan production between an illuminated (open data points) and dark (filled data points) sample. **(D)** Zero order discoloration of the formed formazan illuminated at 81 mW cm^{-2} [O, $R^2 = 0.994$, slope = $(4.18 \pm 0.08) \text{ nM min}^{-1}$] and 53 mW cm^{-2} [□, $R^2 = 0.912$, slope = $(3.4 \pm 0.8) \text{ nM min}^{-1}$].

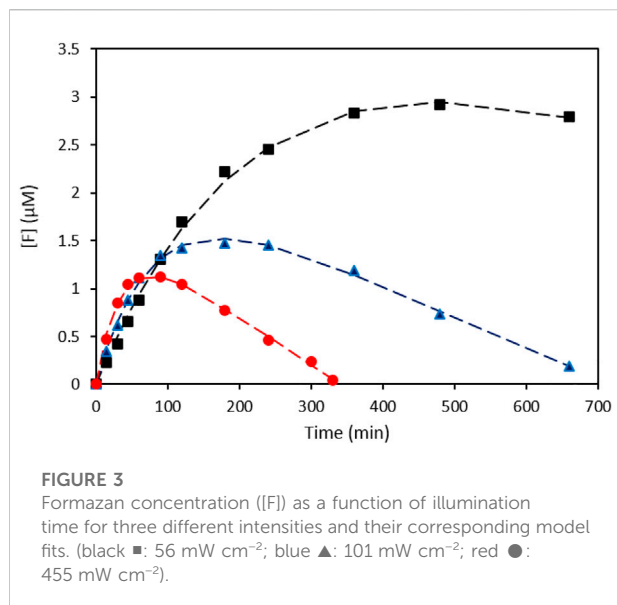
microscopy, elemental analysis, etc.), we kindly refer the reader to our previous publications, as this is not the scope of the present work (Verbruggen et al., 2016).

3.2 XTT probe reaction and kinetic model

In this work, XTT is used to probe plasmonic oxygen activation by a broadband plasmonic rainbow photocatalyst. The experiments are conducted in DMSO, since superoxide is considerably more stable in DMSO compared to water. DMSO is an aprotic solvent that readily deactivates water, thus preventing the unwanted reaction between the superoxide anion radical and any trace amounts of water that may be present (Che et al., 1996; Oritani et al., 2004; Hayyan et al., 2012).

An exploratory assay using the SiO_2 -supported plasmonic catalyst under VIS illumination is shown in Figure 2. The formation of a colored formazan-product with a maximum absorbance at 480 nm is clearly observed (Figure 2A) (Sutherland and Learmonth, 1997; Oritani et al., 2004). The

conversion to the corresponding formazan concentration was achieved by applying Beer's law. Here, the molecular absorption coefficient of XTT-formazan in DMSO at 480 nm was estimated to be $(26.1 \pm 0.3) \cdot 10^3 \text{ M}^{-1} \text{ cm}^{-1}$, based on literature (Paull et al., 1988), after correcting for the solvent. A detailed description of the estimation is given in the supporting information. The time-dependent change in the formazan concentration ([F]) is depicted in Figure 2B. A blank experiment with pristine SiO_2 in a XTT/DMSO solution under illumination showed no XTT to formazan conversion. The reduction of XTT to its colored derivate can therefore be attributed to the presence of the metallic nanoparticles. Interestingly, the bottom curve of Figure 2A shows that already some formazan is formed during sample preparation (*i.e.* even before illumination) invoking the hypothesis that the noble metal bimetallic nanoparticles already have a basal oxygen activation activity, without illumination. This is confirmed for Au nanoparticles in dark by Stowers et al. and Xu et al. (Stowers et al., 2013; Xu et al., 2014) They also observed an additional increase in



oxygen activation by alloying gold and silver. To verify this hypothesis, two additional experiments were performed where one reaction vessel was illuminated, while the other was kept in the dark (Figure 2C). It is clear that formazan is in fact readily formed without illumination, albeit to a far lesser extent than when the sample is illuminated. It can thus be concluded that the visible light induced plasmon excitation improves the oxygen activation efficiency (i.e. O₂⁻ formation) compared to its dark counterpart. These results are in agreement with a study on α-Al₂O₃ supported silver nanocubes (60 nm edge length) by Christopher et al. (Christopher et al., 2011). Due to SPR-mediated oxygen activation, they observed a four-fold increase in the ethylene epoxidation rate when the catalyst was illuminated.

An interesting observation is that in Figures 2A,B the formazan concentration first levels off and subsequently decreases (approximately after 180 min of illumination, black versus red). The stability of the formed formazan under illumination was therefore investigated in more detail. A formazan solution was illuminated at different intensities in the absence of any catalyst. The results are given in Figure 2D, where a zero-order discoloration can be observed.

The observed conversion of XTT to formazan and its subsequent photoinduced discoloration can be described more in detail by a kinetic model. The model is derived in detail in the Supporting Information section, and results in Eq. (1):

$$[F] = ([XTT]_0 - k_3 t) (1 - e^{-k' t}) \quad (1)$$

With [F] the formazan concentration, k_3 a zero-order discoloration rate constant, and k' an apparent first order rate constant, obtained by assuming that that [O₂⁻] >> [XTT]. [F] can

TABLE 1 Parameter values for the model fitted to the experimental formazan formation data.

Intensity [mW cm ⁻²]	k' [min ⁻¹]	k_3 [nM. min ⁻¹]
56	0.004 ± 0.001	3 ± 2
101	0.012 ± 0.001	3.2 ± 0.3
455	0.026 ± 0.004	4.9 ± 0.4

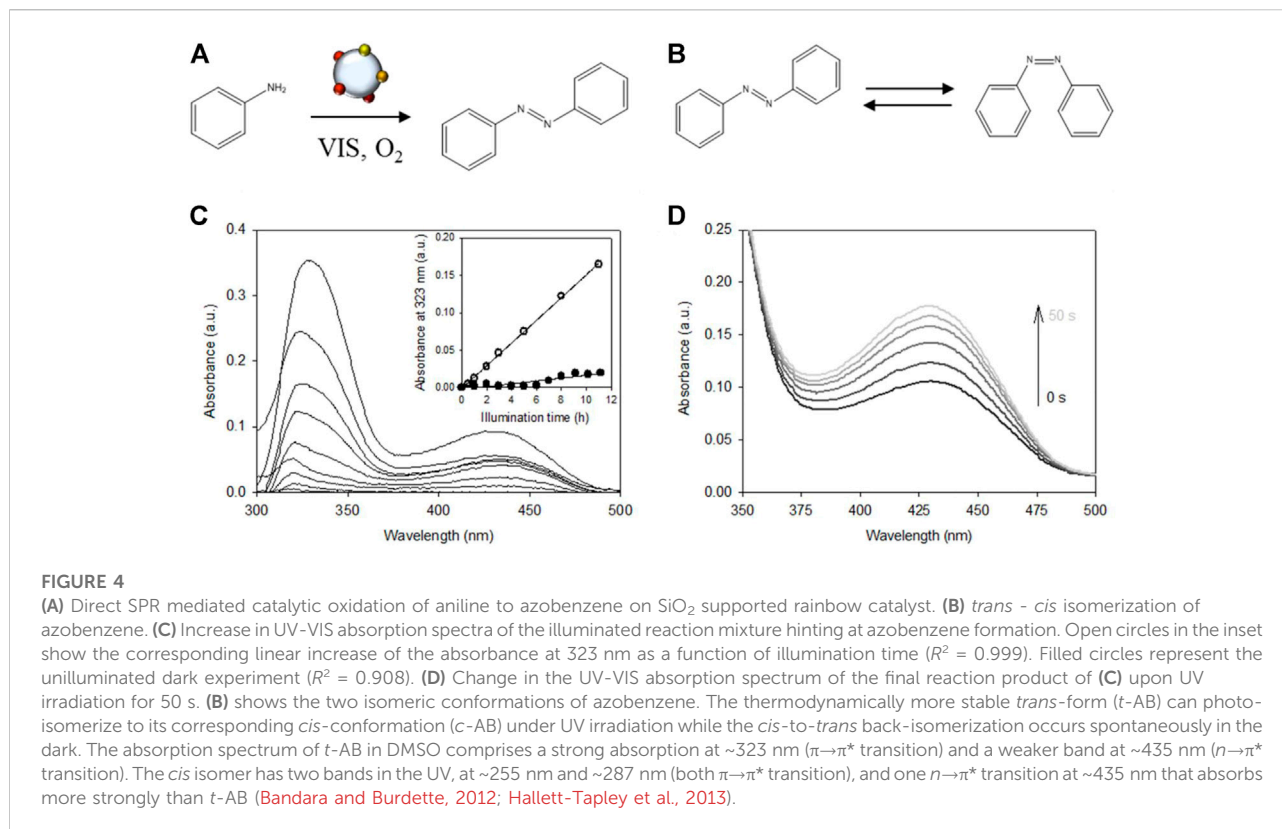
be easily monitored using the absorption band at 480 nm. In addition, assuming no discoloration of the formed formazan would take place, the formazan concentration at $t = \infty$ equals [XTT]₀ as all XTT would be converted into formazan. [XTT]₀ can therefore be substituted by the absorbance of formazan at 480 nm at $t = \infty$ (in the absence of discoloration), ultimately yielding Eq. (2) that can be monitored exclusively based on UV-VIS data.

$$[F] = \frac{Abs_{480 \text{ nm}}(t = t)}{\epsilon_{DMSO, 480 \text{ nm}} \cdot l} = \left(\frac{Abs_{480 \text{ nm}}(t = \infty)}{\epsilon_{DMSO, 480 \text{ nm}} \cdot l} - k_3 t \right) (1 - e^{-k' t}) \quad (2)$$

With $\epsilon_{DMSO, 480 \text{ nm}}$ the estimated molecular absorption coefficient for formazan and l the path length of light through the solution (1 cm).

In Figure 3 the model predictions (dashed lines) are compared to the experimental data for three different experiments performed at varying intensities. The parameters were determined using the Curve Fitting Toolbox application of MATLAB and are shown in Table 1. The obtained R² values were > 0.99 for all the model fits.

Looking at the apparent first order rate constant k' , which can be considered a measure of the oxygen activation rate of the plasmonic rainbow photocatalyst as outlined above, a clear intensity dependence can be observed, as is expected for plasmon-driven photocatalytic reactions (Kale et al., 2014). The calculated rate constants for the zero order formazan discoloration reaction (k_3) in Table 1 are of the same order of magnitude (nM.min⁻¹) as those obtained in the earlier discoloration experiment (Figure 2D) and also display the trend of increasing k_3 value at higher intensities. The combination of both calculated rate constants enables to interpret the peculiar behavior of the curves in Figures 2B, 3: The initial superoxide formation rate is higher at higher illumination intensities, but under these conditions the zero-order discoloration constant also increases. Due to the latter, the formazan concentration sooner reaches a maximum level after which the discoloration reaction dominates at high intensity values. Nonetheless, the excellent fits prove the validity of the kinetic model, which in turn enables to quantitatively evaluate the oxygen activation performance of different plasmonic systems by means of the apparent rate constant k' .



3.3 Plasmon-assisted oxidation of aniline to azobenzene

To demonstrate the oxygen activation capacity of the plasmonic rainbow photocatalyst toward a relevant application, the plasmon-mediated oxidation of aniline to azobenzene under ambient conditions and visible light illumination is studied (Figure 4A), that exists both in a *trans*- and *cis*- configuration (Figure 4B). Aromatic azo compounds have found applications in different branches of industry as dyes, food additives, pigments, pharmaceuticals and precursors for natural product synthesis (Combes and Haveland-Smith, 1982; Kuwabara et al., 1999; Hunger, 2003; Cai et al., 2013; Ghosh et al., 2015). These compounds are conventionally made under high pressure and temperature. In addition, stoichiometric amounts of nitrite salts (entailing high amounts of inorganic salt waste) or environmentally unfriendly oxidants are required (Girrane et al., 2008; Dutta et al., 2016; Peiris et al., 2016). Plasmonic metal nanoparticles provide an ecofriendly and sustainable alternative to these conventional synthesis methods as they allow the reactions to be carried out at less harsh reaction conditions using solely molecular oxygen as oxidant (Girrane et al., 2008; Cai et al., 2013; Ghosh et al., 2015). A recent publication by da Silva et al. has shown that exploiting the plasmonic properties of gold and silver

nanoparticles can lead to additional enhancements in the oxidation of aniline to azobenzene (da Silva et al., 2016).

For the aniline oxidation experiment, the catalyst powder was suspended in an oxygen saturated DMSO solution containing aniline and illuminated with the same visible light source as the one used in the XTT experiment (see Materials and Methods for more details). During the oxidation experiment, the samples showed a clear visual color change of the reaction mixture from colorless to faintly yellow, in accordance with the color of the pure *t*-AB (Figure 4C) (da Silva et al., 2016). The inset in Figure 4C shows that the changes of the most intense band ($\lambda_{\max} \sim 323$ nm) increase linearly with illumination time (open symbols). Similar to the XTT assay, blank measurements using unmodified SiO₂ yielded no appreciable changes to the absorption spectrum. A different blank experiment performed in the presence of the rainbow catalyst but without illumination showed the appearance of the same bands but to a lesser extent (inset Figure 4C, filled symbols). These results agree with the ones obtained in the XTT assay leading to similar conclusions: (i) metal nanoparticles are responsible for the observed reactions and (ii) visible light induced plasmon excitation accelerates the reaction rate. From Figure 4D it can be seen that the absorption band at 435 nm increases under UV illumination. This fully supports *trans*→*cis* azobenzene isomerization

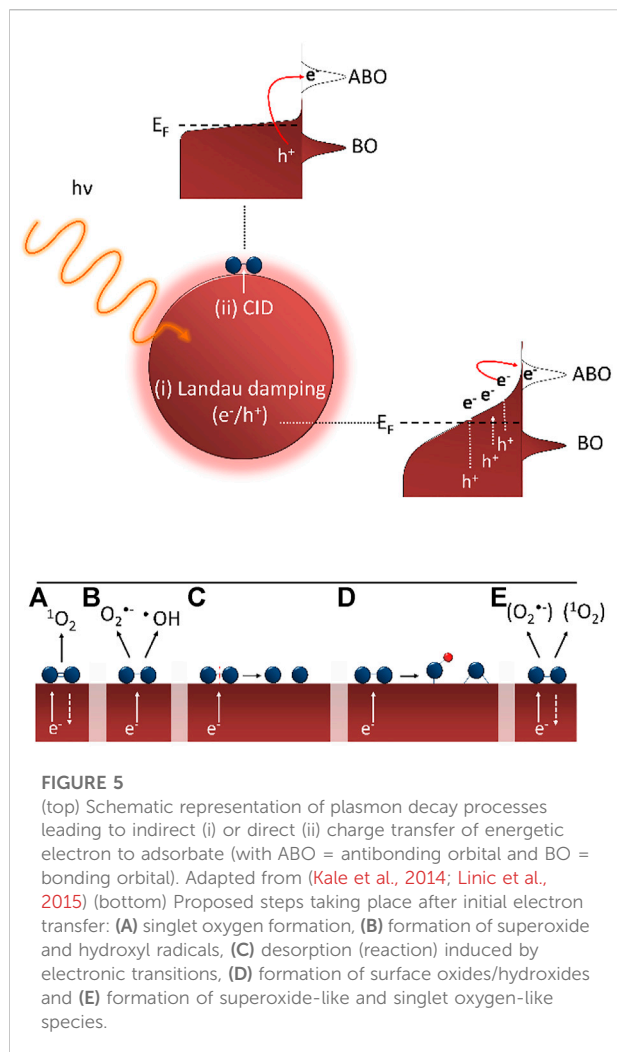


(Figure 4B) as the absorption band at 435 nm of the *cis* isomer absorbs more strongly than *t*-AB. This increase in absorption was also reversible. These results indicate that a plasmon enhanced, noble metal catalyzed oxidative coupling reaction takes place during the performed aniline oxidation experiments. Additional experiments could be conducted to (i) check for possible by-product formation and (ii) quantitatively verify product conversion and selectivity. This, however, is outside the scope of this mere demonstration experiment.

3.4 Mechanistic considerations

Different studies have shown that the first step in the direct oxygen activation on plasmonic nanoparticles is the formation of visible light induced energetic electrons that are subsequently transferred to adsorbed O_2 molecules on the nanoparticle surface. Three main plasmon decay processes can be

discerned: (i) radiative plasmon relaxation, (ii) non-radiative Landau damping resulting in electron-hole pair formation in the metallic nanoparticle and (iii) non-radiative chemical interface damping (CID) where an electron is directly injected in an adsorbate state. The radiative decay mechanism results in the reemission (scattering) of a photon and only becomes important for larger nanoparticles (Evanoff and Chumanov, 2004). The other two mechanisms are schematically represented in Figure 5 (top). The non-radiative Landau damping process results in the formation of energetic charge carriers in the nanoparticle that can in turn lead to chemical reactions on the nanoparticle surface *via* either localized heating or interaction of the formed charge carriers with adsorbed molecules (Linic et al., 2015). For the heating mechanism to have a significant impact on photochemical transformations, high light intensities (several orders of magnitude higher than the solar flux) and small nanoparticles (< 5 nm) are typically required, which is not the case in the present study. In the charge carrier-driven process, energetic charge carriers (electrons) directly interact with adsorbate states, forming transient negative ions (TNI) on the nanoparticle surface. The energetic charge carriers thus transiently interact with unoccupied adsorbate orbitals before the energy is dissipated to the surroundings. The adsorbate-nanoparticle complex is excited, inducing forces on the adsorbate thereby activating it and allowing chemical transformations to occur (Linic et al., 2015). Concerning this charge transfer of energetic electrons from the plasmon excited nanoparticle to the adsorbate, a distinction can be made between an indirect injection process [Landau damping, Figure 5 (i), top] and direct injection mechanism [CID, Figure 5 (ii), top].

The common feature of the abovementioned mechanisms is that plasmon excitation results in the formation of “hot” electrons that can subsequently occupy the antibonding π^* orbital of adsorbed oxygen molecules, forming a TNI. The subsequent steps in this oxygen activation mechanism and the resulting (intermediate) chemical species are still unclear. Vankayala et al. (2011) were the first to observe that singlet oxygen (1O_2) could be formed through plasmonic sensitization on gold, silver and platinum (Figure 5A). This plasmon-induced singlet oxygen formation was also observed by other research groups (Pasparakis, 2013; Gao et al., 2014). Singlet oxygen formation is proposed to be a two-step electron transfer process where first a “hot” SPR excited electron is transiently injected into the antibonding π^* orbital of molecular oxygen, resulting in superoxide anion formation (O_2^-). This TNI subsequently relaxes by back transfer of the electron to the metallic nanoparticle, during which a spin-flip can occur yielding 1O_2 (Vankayala et al., 2013; Gao et al., 2014). In addition to singlet oxygen, Gao et al. (2014) observed superoxide anion and hydroxyl radical formation on plasmon excited gold nanocages using dedicated EPR spin traps (Figure 5A,B). Linic et al. (2015) demonstrated that the

reaction rate of ethylene epoxidation over 50 nm silver cubes is substantially increased under broadband illumination at elevated temperatures. They explained their results through the desorption (reaction) induced by electronic transitions (DIET) mechanism. Plasmon excitation results in the transfer of a “hot” electron into the antibonding orbital forming a TNI. This way energy is deposited in the O-O vibrational mode ultimately dissociating the adsorbed O₂ molecule yielding atomic oxygen (Figure 5C) (Christopher et al., 2011).

The primary step in the reaction mechanism proposed by da Silva et al. (2016) for the SPR mediated oxidation of aniline to azobenzene on gold-silver nanoparticles is the generation of O₂⁻ (da Silva et al., 2016). In our study, the presence of superoxide anions has indeed also been probed by the XTT assay.

4 Conclusion

The direct oxygen activation rate of a broadband plasmonic photocatalyst is evaluated by applying a probe assay based on the reduction of XTT to its corresponding colored formazan by superoxide. The use of an inert nano-SiO₂ support enabled fine dispersion in liquid media, thereby combining advantages of homogeneous and heterogeneous catalysis. Visible light illumination substantially improved the oxygen activation efficiency due to the mediating role of plasmon excitation. A kinetic model is proposed to quantify the oxygen activation efficiency. An excellent match between model and experimental results is obtained. The plasmonic oxygen activation is also demonstrated towards an economic relevant application by monitoring the visible light-induced oxidation of aniline to azobenzene. UV-VIS analysis indicates that *trans*-azobenzene is formed *via* a plasmon-enhanced oxidative coupling reaction, that is commonly thought to proceed *via* intermediary O₂⁻ species. We strongly hope the proposed superoxide probe-assay will become a facile and valuable tool to study also other related (plasmonic) oxygen activation reactions.

Data availability statement

The raw data supporting the conclusions of this article will be made available by the authors, without undue reservation.

References

- Ali, M. E., Rahman, M. M., Sarkar, S. M., and Hamid, S. B. A. (2014). Heterogeneous metal catalysts for oxidation reactions. *J. Nanomater.* 2014, 1–23. doi:10.1155/2014/192038
- Azócar, M. I., Alarcón, R., Castillo, A., Blamey, J. M., Walter, M., and Paez, M. (2019). Capping of silver nanoparticles by anti-inflammatory ligands: Antibacterial activity and superoxide anion generation. *J. Photochem. Photobiol. B Biol.* 193, 100–108. doi:10.1016/j.jphotobiol.2019.02.005
- Bandara, H. M. D., and Burdette, S. C. (2012). Photoisomerization in different classes of azobenzene. *Chem. Soc. Rev.* 41, 1809–1825. doi:10.1039/C1CS15179G

Author contributions

The manuscript was written through contributions of all authors. All authors have given approval to the final version of the manuscript. SV conceived the study. FD, RB, RN, and SV wrote the paper.

Funding

FD (FN 700300002) and SV acknowledge the Research Foundation Flanders (FWO) for financial support through an Aspirant doctoral fellowship.

Acknowledgments

Ir. Maarten Keulemans is greatly thanked for his experimental contribution.

Conflict of interest

The authors declare that the research was conducted in the absence of any commercial or financial relationships that could be construed as a potential conflict of interest.

Publisher's note

All claims expressed in this article are solely those of the authors and do not necessarily represent those of their affiliated organizations, or those of the publisher, the editors and the reviewers. Any product that may be evaluated in this article, or claim that may be made by its manufacturer, is not guaranteed or endorsed by the publisher.

Supplementary material

The Supplementary Material for this article can be found online at: <https://www.frontiersin.org/articles/10.3389/fchem.2022.988542/full#supplementary-material>

- Berridge, M. V., Herst, P. M., and Tan, A. S. (2005). Tetrazolium dyes as tools in cell biology: New insights into their cellular reduction. *Biotechnol. Annu. Rev.* 11, 127–152. doi:10.1016/S1387-2656(05)11004-7

- Boerigter, C., Campana, R., Morabito, M., and Linic, S. (2016). Evidence and implications of direct charge excitation as the dominant mechanism in plasmon-mediated photocatalysis. *Nat. Commun.* 7, 10545. doi:10.1038/ncomms10545

- Brongersma, M. L., Halas, N. J., and Nordlander, P. (2015). Plasmon-induced hot carrier science and technology. *Nat. Nanotechnol.* 10, 25–34. doi:10.1038/nnano.2014.311

- Cai, S., Rong, H., Yu, X., Liu, X., Wang, D., He, W., et al. (2013). Room temperature activation of oxygen by monodispersed metal nanoparticles: Oxidative dehydrogenative coupling of anilines for azobenzene syntheses. *ACS Catal.* 3, 478–486. doi:10.1021/cs300707y
- Campbell, A. N., and Stahl, S. S. (2012). Overcoming the “oxidant problem”: Strategies to use O₂ as the oxidant in organometallic C–H oxidation reactions catalyzed by Pd (and Cu). *Acc. Chem. Res.* 45, 851–863. doi:10.1021/ar2002045
- Che, Y., Tsushima, M., Matsumoto, F., Okajima, T., Tokuda, K., and Ohsaka, T. (1996). Water-induced disproportionation of superoxide ion in aprotic solvents. *J. Phys. Chem.* 100, 20134–20137. doi:10.1021/jp9625523
- Chen, X., Zhu, H. Y., Zhao, J. C., Zheng, Z. F., and Gao, X. P. (2008). Visible-light-driven oxidation of organic contaminants in air with gold nanoparticle catalysts on oxide supports. *Angew. Chem. Int. Ed.* 47, 5353–5356. doi:10.1002/anie.200800602
- Chen, X., Zheng, Z., Ke, X., Jaatinen, E., Xie, T., Wang, D., et al. (2010). Supported silver nanoparticles as photocatalysts under ultraviolet and visible light irradiation. *Green Chem.* 12, 414. doi:10.1039/b921696k
- Chen, K. H., Pu, Y. C., Chang, K. Der, Liang, Y. F., Liu, C. M., Yeh, J. W., et al. (2012). Ag-nanoparticle-decorated SiO₂ nanospheres exhibiting remarkable plasmon-mediated photocatalytic properties. *J. Phys. Chem. C* 116, 19039–19045. doi:10.1021/jp306555j
- Christopher, P., Xin, H. L., and Linic, S. (2011). Visible-light-enhanced catalytic oxidation reactions on plasmonic silver nanostructures. *Nat. Chem.* 3, 467–472. doi:10.1038/nchem.1032
- Combes, R. D., and Haveland-Smith, R. B. (1982). A review of the genotoxicity of food, drug and cosmetic colours and other azo, triphenylmethane and xanthene dyes. *Mutat. Research/Reviews Genet. Toxicol.* 98, 101–243. doi:10.1016/0165-1110(82)90015-X
- Da Silva, A. G. M., Rodrigues, T. S., Wang, J., Yamada, L. K., Alves, T. V., Ornellas, F. R., et al. (2015). The fault in their shapes: Investigating the surface-plasmon-resonance-mediated catalytic activities of silver quasi-spheres, cubes, triangular prisms, and wires. *Langmuir* 31, 10272–10278. doi:10.1021/acs.langmuir.5b02838
- da Silva, A. G. M., Rodrigues, T. S., Correia, V. G., Alves, T. V., Alves, R. S., Ando, R. A., et al. (2016). Plasmonic nanorattles as next-generation catalysts for surface plasmon resonance-mediated oxidations promoted by activated oxygen. *Angew. Chem. Int. Ed.* 55, 7111–7115. doi:10.1002/anie.201601740
- Di, J., Xia, J., Ji, M., Wang, B., Yin, S., Huang, Y., et al. (2016). New insight of Ag quantum dots with the improved molecular oxygen activation ability for photocatalytic applications. *Appl. Catal. B Environ.* 188, 376–387. doi:10.1016/j.apcatb.2016.01.062
- Dingenen, F., Blommaerts, N., Van Hal, M., Borah, R., Arenas-Esteban, D., Lenaerts, S., et al. (2021). Layer-by-layer-stabilized plasmonic gold-silver nanoparticles on TiO₂: towards stable solar active photocatalysts. *Nanomater. (Basel)* 11, 2624. doi:10.3390/nano11102624
- Dutta, B., Biswas, S., Sharma, V., Savage, N. O., Alpay, S. P., and Suib, S. L. (2016). Mesoporous manganese oxide catalyzed aerobic oxidative coupling of anilines to aromatic azo compounds. *Angew. Chem. Int. Ed.* 55, 2171–2175. doi:10.1002/anie.201508223
- Evanoff, D. D., and Chumanov, G. (2004). Size-controlled synthesis of nanoparticles. 2. Measurement of extinction, scattering, and absorption cross sections. *J. Phys. Chem. B* 108, 13957–13962. doi:10.1021/jp0475640
- Gao, L., Liu, R., Gao, F., Wang, Y., Jiang, X., and Gao, X. (2014). Plasmon-mediated generation of reactive oxygen species from near-infrared light excited gold nanocages for photodynamic therapy *in vitro*. *ACS Nano* 8, 7260–7271. doi:10.1021/nn502325j
- Ghosh, S., Acharyya, S. S., Sasaki, T., and Bal, R. (2015). Room temperature selective oxidation of aniline to azoxybenzene over a silver supported tungsten oxide nanostructured catalyst. *Green Chem.* 17, 1867–1876. doi:10.1039/C4GC02123A
- Goto, H., Hanada, Y., Ohno, T., and Matsumura, M. (2004). Quantitative analysis of superoxide ion and hydrogen peroxide produced from molecular oxygen on photoirradiated TiO₂ particles. *J. Catal.* 225, 223–229. doi:10.1016/j.jcat.2004.04.001
- Griirane, A., Corma, A., and García, H. (2008). Gold-catalyzed synthesis of aromatic azo compounds from anilines and nitroaromatics. *Science* 322, 1661–1664. doi:10.1126/science.1166401
- Hallett-Tapley, G. L., D’Alfonso, C., Pacioni, N. L., McTiernan, C. D., González-Béjar, M., Lanzalunga, O., et al. (2013). Gold nanoparticle catalysis of the cis–trans isomerization of azobenzene. *Chem. Commun.* 49, 10073. doi:10.1039/c3cc41669k
- Hayyan, M., Mjalli, F. S., Hashim, M. A., Alnashef, I. M., Al-Zahrani, S. M., and Chooi, K. L. (2012). Long term stability of superoxide ion in piperidinium, pyrrolidinium and phosphonium cations-based ionic liquids and its utilization in the destruction of chlorobenzenes. *J. Electroanal. Chem. (Lausanne)* 664, 26–32. doi:10.1016/j.jelechem.2011.10.008
- Hotze, E. M., Labille, J., Alvarez, P., and Wiesner, M. R. (2008). Mechanisms of Photochemistry and reactive oxygen production by fullerene suspensions in water. *Environ. Sci. Technol.* 42, 4175–4180. doi:10.1021/es702172w
- Huang, Y.-F., Zhang, M., Zhao, L.-B., Feng, J.-M., Wu, D.-Y., Ren, B., et al. (2014). Activation of oxygen on gold and silver nanoparticles assisted by surface plasmon resonances. *Angew. Chem. Int. Ed.* 53, 2353–2357. doi:10.1002/anie.201310097
- Hunger, K. (2003). *Industrial dyes: Chemistry, properties, applications*. Weinheim: Wiley VCH.
- Inoue, T., Fujishima, A., Konishi, S., Honda, K., Zhou, L., Martinez, J. M. P., et al. (2019). Plasmonic effects on CO₂ reduction over bimetallic Ni–Au catalysts. *Chem. Eng. Sci.* 24, 94–104. doi:10.1016/j.ces.2018.04.003
- Kale, M. J., Avanesian, T., and Christopher, P. (2014). Direct photocatalysis by plasmonic nanostructures. *ACS Catal.* 4, 116–128. doi:10.1021/cs400993w
- Kuwabara, T., Nakajima, H., Nanasawa, M., and Ueno, A. (1999). Color change indicators for molecules using methyl red-modified cyclodextrins. *Anal. Chem.* 71, 2844–2849. doi:10.1021/ac9814041
- Lang, X., Chen, X., and Zhao, J. (2014). Heterogeneous visible light photocatalysis for selective organic transformations. *Chem. Soc. Rev.* 43, 473–486. doi:10.1039/C3CS60188A
- Li, Y., Zhang, W., Niu, J., and Chen, Y. (2013). Surface-coating-dependent dissolution, aggregation, and reactive oxygen species (ROS) generation of silver nanoparticles under different irradiation conditions. *Environ. Sci. Technol.* 47, 10293–10301. doi:10.1021/es400945v
- Linic, S., Aslam, U., Boerigter, C., and Morabito, M. (2015). Photochemical transformations on plasmonic metal nanoparticles. *Nat. Mater.* 14, 567–576. doi:10.1038/nmat4281
- Long, R., Mao, K., Gong, M., Zhou, S., Hu, J., Zhi, M., et al. (2014). Tunable oxygen activation for catalytic organic oxidation: Schottky junction versus plasmonic effects. *Angew. Chem. Int. Ed.* 53, 3205–3209. doi:10.1002/anie.201309660
- Oritani, T., Fukuhara, N., Okajima, T., Kitamura, F., and Ohsaka, T. (2004). Electrochemical and spectroscopic studies on electron-transfer reaction between novel water-soluble tetrazolium salts and a superoxide ion. *Inorg. Chim. Acta* 357, 436–442. doi:10.1016/j.ica.2003.05.007
- Pasparakis, G. (2013). Light-induced generation of singlet oxygen by naked gold nanoparticles and its implications to cancer cell phototherapy. *Small* 9, 4130–4134. doi:10.1002/smll.201301365
- Paull, K. D., Shoemaker, R. H., Boyd, M. R., Parsons, J. L., Risbood, P. A., Barbera, W. A., et al. (1988). The synthesis of XTT: A new tetrazolium reagent that is bioreducible to a water-soluble formazan. *J. Heterocycl. Chem.* 25, 911–914. doi:10.1002/jhet.5570250340
- Peiris, S., McMurtrie, J., and Zhu, H.-Y. (2016). Metal nanoparticle photocatalysts: emerging processes for green organic synthesis. *Catal. Sci. Technol.* 6, 320–338. doi:10.1039/C5CY02048D
- Pincella, F., Isozaki, K., and Miki, K. (2014). A visible light-driven plasmonic photocatalyst. *Light. Sci. Appl.* 3, e133. doi:10.1038/lsa.2014.14
- Popescu, T., Lupu, A. R., Raditoiu, V., Purcar, V., and Teodorescu, V. S. (2015). On the photocatalytic reduction of MTT tetrazolium salt on the surface of TiO₂ nanoparticles: Formazan production kinetics and mechanism. *J. Colloid Interface Sci.* 457, 108–120. doi:10.1016/j.jcis.2015.07.005
- Punniyamurthy, T., Velusamy, S., and Iqbal, J. (2005). Recent advances in transition metal catalyzed oxidation of organic substrates with molecular oxygen. *Chem. Rev.* 105, 2329–2364. doi:10.1021/cr050523v
- Robatjazi, H., Bao, J. L., Zhang, M., Zhou, L., Christopher, P., Carter, E. A., et al. (2020). Plasmon-driven carbon–fluorine (C(sp³)-F) bond activation with mechanistic insights into hot-carrier-mediated pathways. *Nat. Catal.* 3, 564–573. doi:10.1038/s41929-020-0466-5
- Sakamoto, H., Ohara, T., Yasumoto, N., Shiraiishi, Y., Ichikawa, S., Tanaka, S., et al. (2015). Hot-electron-induced highly efficient O₂ activation by Pt nanoparticles supported on Ta₂O₅ driven by visible light. *J. Am. Chem. Soc.* 137, 9324–9332. doi:10.1021/jacs.5b04062
- Seidler, E. (1991). The tetrazolium-formazan system: Design and histochemistry. *Prog. Histochem. Cytochem.* 24, 3–79. doi:10.1016/S0079-6336(11)80060-4
- Stowers, K. J., Madix, R. J., and Friend, C. M. (2013). From model studies on Au(111) to working conditions with unsupported nanoporous gold catalysts: Oxygen-assisted coupling reactions. *J. Catal.* 308, 131–141. doi:10.1016/j.jcat.2013.05.033
- Sutherland, M. W., and Learmonth, B. A. (1997). The tetrazolium dyes MTS and XTT provide new quantitative assays for superoxide and superoxide dismutase. *Free Radic. Res.* 27, 283–289. doi:10.3109/10715769709065766
- Swearer, D. F., Zhao, H., Zhou, L., Zhang, C., Robatjazi, H., Martinez, J. M. P., et al. (2016). Heterometallic antenna–reactor complexes for photocatalysis. *Proc. Natl. Acad. Sci. U. S. A.* 113, 8916–8920. LP – 8920. doi:10.1073/pnas.1609769113
- Turkevich, J., Stevenson, P. C., and Hillier, J. (1951). A study of the nucleation and growth processes in the synthesis of colloidal gold. *Discuss. Faraday Soc.* 11, 55. doi:10.1039/DF9511100055

- Vankayala, R., Sagadevan, A., Vijayaraghavan, P., Kuo, C. L., and Hwang, K. C. (2011). Metal nanoparticles sensitize the formation of singlet oxygen. *Angew. Chem. Int. Ed.* 50, 10640–10644. doi:10.1002/anie.201105236
- Vankayala, R., Kuo, C.-L., Sagadevan, A., Chen, P.-H., Chiang, C.-S., Hwang, K. C., et al. (2013). Morphology dependent photosensitization and formation of singlet oxygen ($^1\Delta_g$) by gold and silver nanoparticles and its application in cancer treatment. *J. Mater. Chem. B* 1, 4379. doi:10.1039/c3tb20806k
- Verbruggen, S. W., Keulemans, M., Goris, B., Blommaerts, N., Bals, S., Martens, J. A., et al. (2016). Plasmonic “rainbow” photocatalyst with broadband solar light response for environmental applications. *Appl. Catal. B Environ.* 188, 147–153. doi:10.1016/j.apcatb.2016.02.002
- Wang, F., Li, C., Chen, H., Jiang, R., Sun, D., Li, Q., et al. (2013). Plasmonic harvesting of light energy for suzuki coupling reactions. *J. Am. Chem. Soc.* 135, 5588–5601. doi:10.1021/ja310501y
- Wang, J. L., Ando, R. A., and Camargo, P. H. C. C. (2014). Investigating the plasmon-mediated catalytic activity of AgAu nanoparticles as a function of composition: Are two metals better than one? *ACS Catal.* 4, 3815–3819. doi:10.1021/cs501189m
- Wang, J., Ando, R. A., and Camargo, P. H. C. (2015). Controlling the selectivity of the surface plasmon resonance mediated oxidation of p -aminothiophenol on Au nanoparticles by charge transfer from UV-excited TiO₂. *Angew. Chem. Int. Ed. Engl.* 127, 7013–7016. doi:10.1002/ange.201502077
- Wen, T., Zhang, H., Chong, Y., Wamer, W. G., Yin, J. J., and Wu, X. (2016). Probing hydroxyl radical generation from H₂O₂ upon plasmon excitation of gold nanorods using electron spin resonance: Molecular oxygen-mediated activation. *Nano Res.* 9, 1663–1673. doi:10.1007/s12274-016-1060-7
- Wittstock, A., Zielasek, V., Biener, J., Friend, C. M., and Baumer, M. (2010). Nanoporous gold catalysts for selective gas-phase oxidative coupling of methanol at low temperature. *Science* 327, 319–322. doi:10.1126/science.1183591
- Wu, X., Jaatinen, E., Sarina, S., and Zhu, H. Y. (2017). Direct photocatalysis of supported metal nanostructures for organic synthesis. *J. Phys. D: Appl. Phys.* 50, 283001. doi:10.1088/1361-6463/aa73f6
- Xiao, Q., Jaatinen, E., and Zhu, H. (2014a). Direct photocatalysis for organic synthesis by using plasmonic-metal nanoparticles irradiated with visible light. *Chem. Asian J.* 9, 3046–3064. doi:10.1002/asia.201402310
- Xiao, Q., Sarina, S., Jaatinen, E., Jia, J., Arnold, D. P., Liu, H., et al. (2014b). Efficient photocatalytic Suzuki cross-coupling reactions on Au–Pd alloy nanoparticles under visible light irradiation. *Green Chem.* 16, 4272–4285. doi:10.1039/C4GC00588K
- Xu, B., Siler, C. G. F., Madix, R. J., and Friend, C. M. (2014). Ag/Au mixed sites promote oxidative coupling of methanol on the alloy surface. *Chem. Eur. J.* 20, 4646–4652. doi:10.1002/chem.201304837
- Xue, W., Lin, Z., Chen, H., Lu, C., and Lin, J.-M. (2011). Enhancement of ultraweak chemiluminescence from reaction of hydrogen peroxide and bisulfite by water-soluble carbon nanodots. *J. Phys. Chem. C* 115, 21707–21714. doi:10.1021/jp207554t
- Yamakoshi, Y., Umezawa, N., Ryu, A., Arakane, K., Miyata, N., Goda, Y., et al. (2003). Active oxygen species generated from photoexcited fullerene (C₆₀) as potential medicines: O₂^{•-} versus ¹O₂. *J. Am. Chem. Soc.* 125, 12803–12809. doi:10.1021/ja0355574
- Yu, S., and Jain, P. K. (2019). Plasmonic photosynthesis of C₁–C₃ hydrocarbons from carbon dioxide assisted by an ionic liquid. *Nat. Commun.* 10, 2022. doi:10.1038/s41467-019-10084-5
- Zhang, X., Ke, X., and Zhu, H. (2012). Zeolite-supported gold nanoparticles for selective photooxidation of aromatic alcohols under visible-light irradiation. *Chem. Eur. J.* 18, 8048–8056. doi:10.1002/chem.201200368
- Zhang, Y., Xiao, Q., Bao, Y., Zhang, Y., Bottle, S., Sarina, S., et al. (2014). Direct photocatalytic conversion of aldehydes to esters using supported gold nanoparticles under visible light irradiation at room temperature. *J. Phys. Chem. C* 118, 19062–19069. doi:10.1021/jp505552v
- Zhang, X., Li, X., Zhang, D., Su, N. Q., Yang, W., Everitt, H. O., et al. (2017). Product selectivity in plasmonic photocatalysis for carbon dioxide hydrogenation. *Nat. Commun.* 8, 14542. doi:10.1038/ncomms14542
- Zhao, L. B., Zhang, M., Huang, Y. F., Williams, C. T., Wu, D. Y., Ren, B., et al. (2014). Theoretical study of plasmon-enhanced surface catalytic coupling reactions of aromatic amines and nitro compounds. *J. Phys. Chem. Lett.* 5, 1259–1266. doi:10.1021/jz5003346
- Zhao, L. Bin, Liu, X. X., Zhang, M., Liu, Z. F., Wu, D. Y., and Tian, Z. Q. (2016). Surface plasmon catalytic aerobic oxidation of aromatic amines in metal/molecule/metal junctions. *J. Phys. Chem. C* 120, 944–955. doi:10.1021/acs.jpcc.5b07966
- Zhou, L., Martirez, J. M. P., Finzel, J., Zhang, C., Swearer, D. F., Tian, S., et al. (2020). Light-driven methane dry reforming with single atomic site antenna-reactor plasmonic photocatalysts. *Nat. Energy* 5, 61–70. doi:10.1038/s41560-019-0517-9
- Zhou, L., Lou, M., Bao, J. L., Zhang, C., Liu, J. G., Martirez, J. M. P., et al. (2021). Hot carrier multiplication in plasmonic photocatalysis. *Proc. Natl. Acad. Sci. U. S. A.* 118, e2022109118–6. doi:10.1073/pnas.2022109118
- Zhu, H., Chen, X., Zheng, Z., Ke, X., Jaatinen, E., Zhao, J., et al. (2009). Mechanism of supported gold nanoparticles as photocatalysts under ultraviolet and visible light irradiation. *Chem. Commun.* 48, 7524–7526. doi:10.1039/b917052a
- Zhu, H., Ke, X., Yang, X., Sarina, S., and Liu, H. (2010). Reduction of nitroaromatic compounds on supported gold nanoparticles by visible and ultraviolet light. *Angew. Chem. Int. Ed.* 49, 9657–9661. doi:10.1002/anie.201003908